

# 't Hooft's Polygon Approach Hyperbolically Revisited

**Helia R. Hollmann<sup>1</sup> and Ruth M. Williams<sup>2</sup>**

Department of Applied Mathematics and Theoretical Physics,  
Silver Street, Cambridge CB3 9EW, England

## Abstract

The initial data in the polygon approach to (2+1)D gravity coupled to point particles are constrained by the vertex equations and the particle equations. We establish the hyperbolic nature of the vertex equations and derive some consequences. In particular we are able to identify the hyperbolic group of motions as discrete analogues of the diffeomorphisms in the continuum theory. We show that particles can be included “hyperbolically” as well, but they spoil the gauge invariance. Finally we derive consistent sets of initial data.

---

<sup>1</sup>e-mail: H.Hollmann@damtp.cam.ac.uk

<sup>2</sup>e-mail: R.M.Williams@damtp.cam.ac.uk

# 1 Introduction

As a response to a paper by Gott [2] establishing acausal features in (2+1)D gravity coupled to point particles, 't Hooft invented his polygon approach [9]. He succeeded in showing that even in the case of two particles of equal mass and rapidity approaching each other nearly head-on, the space-time would have to undergo a big crunch before a closed timelike curve could be formed.

His idea to split the space-time into a direct product of a cosmological time and a Cauchy surface tessellated by entirely flat polygons turned out to be a particularly useful approach to describe particles in a (2+1)D gravity theory. In the last couple of years toy models have been constructed [6], [10], issues of topology have been addressed [15], [6], particle decay and space-time kinematics have been investigated [16], and inspired by the polygon approach quantized models of (2+1)D space-time have been invented [11], [13], [4].

As a (2+1)D theory of gravity has very peculiar features we do not claim that we study the theory in order to get any particular insight into the (3+1)D equivalent. Due to the fact that in (2+1)D the Riemannian curvature tensor is algebraically dependent on the energy momentum tensor the space-time is locally flat outside the sources. In the case of pure gravity topology might introduce a certain degree of nontriviality. There an open neighbourhood isometric to Minkowski space cannot be extended to include all of the manifold because of nontrivial gluing homomorphisms. If we include particles, we are confronted with the fact that the theory has no Newtonian limit. Test particles in a Newtonian theory experience a logarithmic gravitational potential outside the matter sources and hence accelerate. In an alternative classical or a quantum theory of gravity one would certainly like to test the results against the classical theory or to establish some kind of classical limit. Here this is not possible. But let us follow 't Hooft's ideas more closely. His approach – roughly speaking – is an implementation of the local flatness of space-time in the pure gravity scenario supplemented by the additional conelike structure introduced by particles. Again, in (3+1)D gravity a particle would not simply cut a cone out of space-time.

What are our motivations? We would like to address two issues mainly. First of all (2+1)D gravity coupled to point particles is interesting in its own right. In particular it is a nontrivial task to follow the time evolution of a (2+1)D space-time with particles. The system has finitely many degrees of freedom but – as is well known – even for a four particle system the analytical solution is not known in classical mechanics. Therefore we would like to perform a computer simulation of particle universes tessellated by polygons. 't Hooft himself [10] wrote a computer program to evolve point particles in (2+1)D. Unfortunately he implemented the code on a very small (40 kbytes memory) and old home computer. Somehow the code does not seem to be transferable to a modern machine. His big bang and big crunch hypothesis as well as other results [10] are based on a 1-polygon tessellated Cauchy surface with either  $S^2$

or  $S^1 \times S^1$  topology. We would like to test them against more complex initial configurations. Furthermore there are several approaches to (2+1)D gravity with and without particles, under discussion. We aim at comparing several of them, starting with the polygon approach and Regge calculus. This paper is a step in both directions.

We start by reviewing the basic setup for the polygon approach to make the paper sufficiently self-contained. Then we first investigate the pure gravity sector the initial data of which is described by the so called vertex equations. Already 't Hooft [12] noticed that these equations are related to trigonometric properties of triangles in a hyperbolic space. We establish this relation in detail proving that the vertex relations can be reduced to the hyperbolic law of sines and the first and second law of hyperbolic cosines. The laws of sines and cosines for the edges can be derived from the law of cosines for the angles, leading to the result that only one equation out of the set of vertex relations is independent. We decided to take the hyperbolic point of view seriously. This leads to interesting consequences. A close investigation of the vertex relations then yields the result that it is the freedom to choose frames which make the hyperbolic configurations possible. As a next step we establish the hyperbolic nature of a particle vertex. The particle equations turn out to be the trigonometric relations in a rectangular hyperbolic triangle. Of course, here the hyperbolic geometry cannot disappear by a gauge transformation. In the last chapter we summarize some of the consistent initial configurations we have found.

## 2 Pure Gravity Sector

Let the (2+1)D space-time be foliated by two-dimensional cauchy surfaces. We use the feature that vacuum space-time is entirely flat and tessellate the spatial part of it by polygonal tiles. To each of these pieces of  $\mathbb{R}^2$  we attach a Lorentz frame. We impose two further constraints. First, let us assume that time runs equally fast for all the polygons, i.e. they have a common clock. This corresponds to partially fixing the gauge. Secondly we consider 3-valent vertices only. This does not impose restrictions on the physics of our system as all other configurations can be decomposed into configurations with 3-valent vertices and edges with zero length connecting them.

The consequences of these assumptions are proven in [9] (we call them “initial consequences” in the following): The lengths of adjacent edges measured in the reference frame of each polygon are equal. The velocity of the edges turns out to be orthogonal to the orientation of the edges viewed in the rest frame of one polygon as well as with respect to the other polygon’s frame. They are equal up to signs.

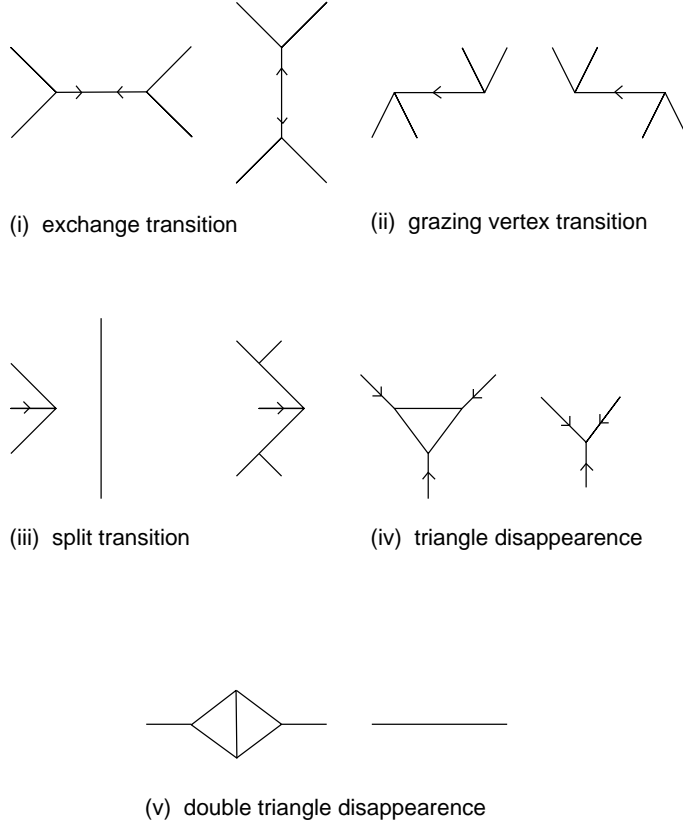


**figure 1:** pure gravity transitions

For reasons of consistency these features have to be valid at every instant of time leading to so called transition rules (see **figure 1**) which have been classified by 't Hooft [10]. The transition rules have to be taken into account whenever the polygonal configuration changes.

In the vacuum case this is happening when one or more edges shrink to zero or a vertex hits an edge leading to an intermediate configuration of several 3-valent vertices connected by edges of zero length. As the edges “carry” a velocity their lengths will change in time. There is a growth rate associated with every vertex. That results in time evolution equations for the edge lengths  $L_1$  and  $L_2$  of the straight lines between the vertices  $A$  and  $B$  or  $A$  and  $C$ , respectively. The rate of change of the  $L_i$ 's in time is given by

$$\dot{L}_1 = g_{A,1} + g_{B,1}, \quad \dot{L}_2 = g_{A,2} + g_{C,2}.$$

$g_{A,1}, g_{A,2}, g_{B,1}, g_{C,2}$  are the growth rates associated with the vertices  $A, B, C$  and the edge lengths  $L_1$  and  $L_2$ , respectively. Let us focus on the vertex  $A$  as shown in **figure 2**. The growth rates  $g_{A,1}$  and  $g_{A,2}$  are read off to be

$$g_{A,1} = \frac{v_2 + v_1 \cos \alpha_3}{\sin \alpha_3}, \quad g_{A,2} = \frac{v_1 + v_2 \cos \alpha_3}{\sin \alpha_3}.$$

$g_{B,1}$  and  $g_{C,2}$  are calculated in an analogous manner.

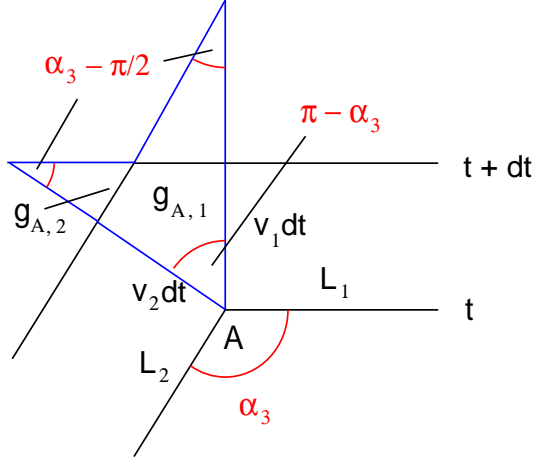


**figure 2:** equations of motion for gravity vertices

From an algorithmic point of view evolution of a polygon universe in pure gravity means the following: we start with a proper set of initial data, that is a number of polygons, the coordinates of their vertices (and therefore the length of the edges joining them) and the velocities with which they move. We then let the configuration evolve linearly until a transition takes place. The transition rules reshuffle the set of initial data into another one, which has in general a different number of polygons, edges and vertices still obeying the initial conditions. The initial data cannot be chosen freely.

At the edges, the frames of adjacent polygons are related by a Lorentz transformation. Let us circle around a vertex, which is a meeting point of three polygons and therefore of three reference frames. To circle around a vertex means to undergo a sequence of Lorentz boosts in the  $tx$ -plane with boost parameters  $2\eta_i$  and subsequent rotations with angles  $\alpha_i$  in the  $xy$ -plane. Assuming a counterclock-wise orientation they combine to the following identity due to the flatness of space-time

$$L_2 R_3 L_1 = R_1^{-1} L_3^{-1} R_2^{-1},$$

with

$$R_i = \begin{pmatrix} 1 & 0 & 0 \\ 0 & \cos \alpha_i & \sin \alpha_i \\ 0 & -\sin \alpha_i & \cos \alpha_i \end{pmatrix} \quad \text{and} \quad L_i = \begin{pmatrix} \cosh 2\eta_i & \sinh 2\eta_i & 0 \\ \sinh 2\eta_i & \cosh 2\eta_i & 0 \\ 0 & 0 & 1 \end{pmatrix}.$$

In detail the equations are

$$\text{ch}_3 = \text{ch}_1 \text{ch}_2 + \text{c}_3 \text{sh}_1 \text{sh}_2 \quad (1a)$$

$$-\text{c}_2 \text{sh}_3 = \text{ch}_2 \text{sh}_1 + \text{c}_3 \text{ch}_1 \text{sh}_2 \quad (1b)$$

$$\text{s}_2 \text{sh}_3 = \text{sh}_2 \text{s}_3 \quad (1c)$$

$$-\text{c}_1 \text{sh}_3 = \text{ch}_1 \text{sh}_2 + \text{c}_3 \text{ch}_2 \text{sh}_1 \quad (1d)$$

$$c_1 c_2 ch_3 - s_1 s_2 = sh_1 sh_2 + c_3 ch_1 ch_2 \quad (1e)$$

$$-c_1 s_2 ch_3 - s_1 c_2 = s_3 ch_2 \quad (1f)$$

$$-s_1 sh_3 = -s_3 sh_1 \quad (1g)$$

$$s_1 c_2 sh_3 + c_1 s_2 = -s_3 ch_1 \quad (1h)$$

$$-s_1 s_2 ch_3 + c_1 c_2 = c_3 \quad (1i)$$

$s_i, c_i$  denote  $\sin \alpha_i, \cos \alpha_i$  and  $sh_i, ch_i$  are  $\sinh 2\eta_i, \cosh 2\eta_i$ . By taking into account the permutation of indices or by fixing one index and interchanging the other two<sup>3</sup>, we find that (1a) is equivalent to (A.5), (1c) and (1g) correspond to (A.2), (1f) and (1h) are (A.3) and (1i) leads to (A.4). (A.2) – (A.5) refer to 't Hooft's notation in [9]. For the convenience of the reader we include his equations here.

$$s_1 : s_2 : s_3 = sh_1 : sh_2 : sh_3 \quad (A.2)$$

$$ch_2 s_3 + s_1 c_2 + c_1 s_2 ch_3 = 0 \quad (A.3)$$

$$c_1 = c_2 c_3 - ch_1 s_2 s_3 \quad (A.4)$$

$$ch_1 = ch_2 ch_3 + sh_2 sh_3 c_1 \quad (A.5)$$

$$\cot_2 = -\cot_1 ch_3 - \frac{\coth_2 sh_3}{s_1} \quad (A.6)$$

(1b) and (1d) are equivalent. They arise using the identity  $s_i = c sh_i^4$  with cyclic permutations from (A.3). That equation (1e) is not independent can be seen in the following manner: we start with

$$s_1 s_2 sh_3^2 = s_3^2 sh_1 sh_2 .$$

Equivalently we get

$$ch_3 c_3 + ch_3^2 s_1 s_2 - s_1 s_2 = ch_3 c_3 - c_3^2 sh_1 sh_2 + sh_1 sh_2 .$$

With (1i) and (1a) we derive

$$ch_3 c_1 c_2 - s_1 s_2 = c_3 ch_1 ch_2 + sh_1 sh_2 ,$$

which is equation (1e).

As the next step we show that at most only two of 't Hooft's equations, (A.2) and (A.5), are independent. We already got the result that (1d) is a consequence of (A.2) and (A.3), and (1e) follows with (A.2), (A.3) and (A.5). Therefore it is sufficient to show that (A.3) and (A.4) can be derived using (A.2) and (A.5). Indeed, if we start with a cyclic permutation of (A.5) we find

$$ch_2 = ch_3 ch_1 + c_2 sh_1 sh_3 = ch_3(ch_2 ch_3 + c_1 sh_2 sh_3) + c_2 sh_1 sh_3 .$$

This is equivalent to

$$0 = sh_3 (sh_3 ch_2 + c_1 sh_2 ch_3 + c_2 sh_1) .$$

---

<sup>3</sup>that is, we change the orientation of the rotations

<sup>4</sup>which is given by the vertex equations (1c) and (1g), respectively:  $c = s_j / sh_j$

(A.3) follows by using (A.2). On the other hand, if we begin our calculations with (A.3) with indices 2 and 3 interchanged and substitute this into (A.3) we derive (A.4) with indices 1 and 2 interchanged.

In addition to the equations (A.2) – (A.5), 't Hooft uses the equation (A.6) which is a combination of (A.2) and (A.3).

To summarize these results let us now replace the angle  $\alpha$  by  $\pi - \alpha$ . Then the equations (A.4) and (A.5) become

$$s_2 s_3 \operatorname{ch}_1 = c_2 c_3 + c_1 \quad (\text{A.4}')$$

$$\operatorname{ch}_1 = \operatorname{ch}_2 \operatorname{ch}_3 - c_1 \operatorname{sh}_2 \operatorname{sh}_3 \quad (\text{A.5}')$$

We identify [1] (A.5') with the first law and (A.4') with the second law of hyperbolic cosines. (A.2) is the law of hyperbolic sines. But we succeed in showing even more: (A.2) and (A.5) are a consequence of (A.4). That is due to the fact that in hyperbolic geometry the cosine and sine formulas are not independent of each other. The laws of hyperbolic sines and cosines for the edges can be derived from the law of cosines for the angles.

Let us first prove that (A.2) follows with (A.4). Let  $s_2 s_3$  be unequal to zero. The case  $s_2 s_3$  equal to zero is governed by the so called trivial and quasistatic vertices, which we discuss below. We can write

$$\operatorname{sh}_1^2 = \operatorname{ch}_1^2 - 1 = \frac{(c_2 c_3 - c_1)^2}{s_2^2 s_3^2} - \frac{(1 - c_2^2)(1 - c_3^2)}{s_2^2 s_3^2}.$$

Consequently the following equation holds by a cyclic permutation

$$s_2^2 s_3^2 \operatorname{sh}_1^2 = c_1^2 + c_2^2 + c_3^2 - 1 - 2 c_1 c_2 c_3 = s_1^2 s_3^2 \operatorname{sh}_2^2$$

and therefore we find

$$\frac{\operatorname{sh}_1^2}{\operatorname{sh}_2^2} = \frac{s_1^2}{s_2^2} \quad \text{and} \quad \frac{\operatorname{sh}_1}{\operatorname{sh}_2} = \pm \frac{s_1}{s_2}.$$

Next we show that (A.5) follows from (A.2) and (A.4). We assume that  $s_1 s_2 s_3$  is unequal to zero.

$$\begin{aligned} \operatorname{ch}_1 - \operatorname{ch}_2 \operatorname{ch}_3 &= \frac{c_2 c_3 - c_1}{s_2 s_3} - \frac{(c_1 c_3 - c_2)(c_1 c_2 - c_3)}{s_1^2 s_2 s_3} \\ &= c_1 \left( \frac{-1 - 2 c_1 c_2 c_3 + c_1^2 + c_2^2 + c_3^2}{s_1^2 s_2 s_3} \right) \\ &= \frac{c_1 s_2^2 s_3^2 \operatorname{sh}_1^2}{s_1^2 s_2 s_3} = \frac{c_1 s_2 s_3 \operatorname{sh}_1^2}{s_1^2} = c_1 \operatorname{sh}_2 \operatorname{sh}_3 \end{aligned}$$

and therefore

$$\operatorname{ch}_1 - \operatorname{ch}_2 \operatorname{ch}_3 = c_1 \operatorname{sh}_2 \operatorname{sh}_3.$$

We have proved that the vertex equations introduced by 't Hooft are not an independent set of equations. They can be reduced to one equation. They

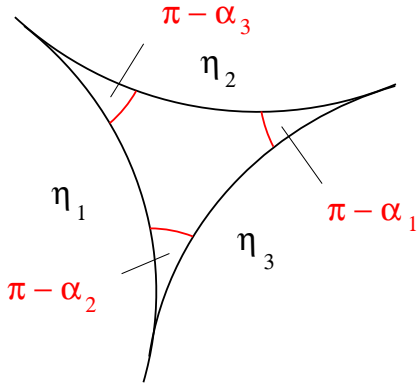


**figure 3a:** The hyperbolic triangle.

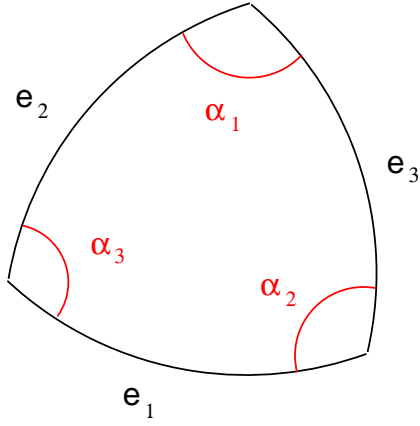


**figure 3b:** The elliptic triangle.

are nothing but the defining relation of a triangle in hyperbolic space. The inner angles of the triangle are  $\pi - \alpha_i$ , where  $\alpha_i$  are the angles between the edges meeting at a 3-valent vertex. The edges of the triangles are given by the boost parameters  $2\eta_i$ . Whereas in hyperbolic geometry the edge length of the triangles are assumed to be greater than zero, that is no longer the case here. The  $\eta_i$ 's can be positive or negative.

The axioms of hyperbolic geometry immediately lead to the consequence that the sum of the inner angles in a triangle is less than  $\pi$ . Triangles which are similar are already congruent. If the configuration is “truly hyperbolic”, that is  $\sum(\pi - \alpha_i) < \pi$  then we conclude that  $\sum \alpha_i > 2\pi$  and the geometry of our polygons is elliptic. If the angles do not add up to  $2\pi$ , we get the result that – still imposing a flat configuration – the edges are not represented by straight lines. For hyperbolic configurations we use for purposes of illustration the Poincaré model on the open unit disk. In this manner the straight lines forming a Euclidean triangle get replaced by segments of circles (see **figure 3a**). The circles have the property that they intersect the unit circle orthogonally. For elliptic geometry it is still possible to use segments of circles but the pieces which build up a triangle or a more general polygon are concave rather than convex (see **figure 3b**).

One particular solution of the vertex equations, which exists for a given deficit angle  $\beta, 0 \leq \beta < \pi$ , involves equilateral hyperbolic triangles. The angles  $\alpha_1 = \alpha_2 = \alpha_3 = \alpha$  and the boosts  $\eta_1 = \eta_2 = \eta_3 = \eta$  fulfil the vertex equations. To every hyperbolic triangle there corresponds a vertex (see **figure 4**). As mentioned above the angles of the hyperbolic triangle are  $\pi - \alpha_i, 1 \leq i \leq 3$ , and  $\sum(\pi - \alpha_i) < \pi$ . Consequently the angles at a vertex add up to  $\sum \alpha_i > 2\pi$ . In particular, they do not add up to  $2\pi$  and the edges cannot be represented by straight lines. The overlap of the angles is given by the deficit angle. The edges are represented by segments of a circle, which carry a boost vector.

‘t Hooft’s vertex equations involve angles and the boost parameters of the Lorentz transformation. The equations of motion tell us how the lengths of

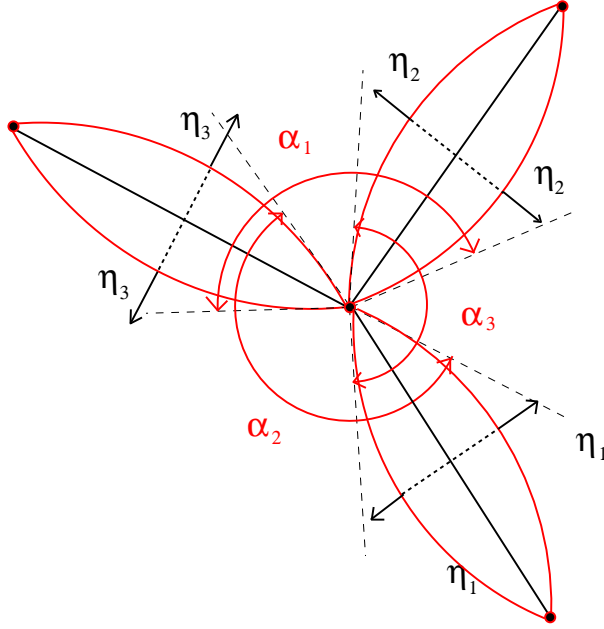


figure 4: The moving vertex

the edges change with time. Nevertheless coordinates are not only necessary to set up a proper initial configuration but in addition if a vertex (later on also a particle) hits an edge and a transition takes place. To get the positions of the newly formed edges, coordinates and in particular a parametrization of the edges are needed. We continue to interpret the edge length in a Euclidean manner. Given two vertices  $p_1, p_2$  the straight line  $\overline{p_1 p_2}$  joining them is the length of the edge which is described by a circle segment through  $p_1$  and  $p_2$ .

If the angles  $\alpha_i$  add up to  $2\pi$ , we are back in Euclidean geometry. Then the edges are straight lines.

In this case we find two distinct configurations. Either  $\eta_1 = \eta_2 = \eta_3 = 0$  or  $\eta_2 = 0$  and  $\eta_1 = \eta_3 = \eta$  (and permutations). The former case is known as “trivial vertex” in the literature [16]. At a “trivial vertex” the angles  $\alpha_1, \alpha_2$ , and  $\alpha_3$  can be chosen arbitrarily. It is a special case of the latter one which is called the “quasistatic vertex” (see [16]). Let us demonstrate this with equation (1i):  $c_3 = c_1 c_2 - s_1 s_2 \text{ch}_3$ . For  $c_3$  we have  $c_3 = \cos(2\pi - \alpha_1 - \alpha_2) = c_1 c_2 - s_1 s_2$ . Therefore either  $s_1 s_2 = 0$  or  $\text{ch}_3 = 1$ . In the former case we get by a cyclic permutation of (1i) that either all of the velocities vanish or the vertex is a quasistatic one.

The latter case only contains the quasistatic vertex. If one of the rapidities, say  $\eta_1$ , vanishes and the other two are equal the angles cannot be chosen freely.  $\alpha_1$  is equal to  $\pi$ ,  $\alpha_2 = \alpha$  and  $\alpha_3$  turns out to be  $\pi - \alpha$ .

The Euclidean configurations lead us to the interpretation of the non-Euclidean

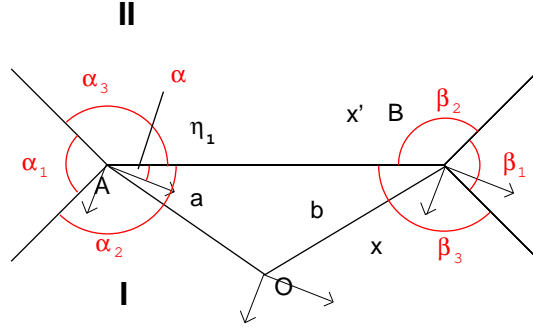


**figure 5:** Matching of vertices

ones. Whenever we choose one of the  $\eta$ 's to be equal to zero the configuration is a Euclidean one. As nothing prevents us from doing so the hyperbolic configurations turn out to be pure gauge. They are not all of the possible gauge transformations as we initially fixed the gauge partially by setting  $g_{00} = 1$ . As an aside we remark that in order to extract physical information like the energy of the polygon universe we have to transform our tessellated surface to one common frame.

Let us make a Gedanken experiment. Assume that there is exactly one coordinate system attached to every polygon. Assume further that the coordinate systems of two polygons say **I**, **II** (see **figure 5**) transform into each other. We use the transformation procedure described above. Then the vertices cannot be treated in isolation in the polygon approach. The data which are connected with a vertex – the angles and the boost velocities – tell us how to perform a coordinate transformation from one polygon to another one across a common edge. Let us consider the situation shown in **figure 5**. Let  $O$  be the origin of frame **I** and **II**. We now perform the transformation across the edge  $\overline{AB}$  in two ways. At first we go via  $A$ . Let us assume that the coordinate axis makes an angle  $\alpha$  with the edge  $\overline{AB}$ . Another possibility is to go via  $B$ . Let us assume that the frame axes and  $\overline{AB}$  there enclose an angle  $\beta$ . The two ways of performing the transformation of points  $x$  in frame **I** to points  $x'$  in frame **II** must yield the same result.

Let us start with a frame attached to  $A$  denoted by the “ $A$ -frame” in the following. A transformation from **I** to **II** means rotating by an angle  $\alpha_3$  and applying a boost with parameter  $2\eta_1$ :

$$x' = R_{-\alpha} R_{\alpha_3} L_1 R_{\alpha} x.$$

If we attach the same frame to  $B$  (called the  $B$ -frame) it follows that

$$\bar{x}' = R_{-\alpha} R_{\beta_2} L_1 R_{\alpha} \bar{x}.$$

Points  $x$  measured in the  $A$ -frame have to be transformed into points  $\bar{x}$  in the  $B$ -frame and vice versa

$$\bar{x} = x + a - b, \quad x = \bar{x} + b - a,$$

where  $a$  and  $b$  denote the vectors  $\overline{OA}$  and  $\overline{OB}$ , respectively. We now describe the movements in the  $B$ -frame as seen with respect to the  $A$ -frame. Take a point  $x$  in the  $A$ -frame, transform it first to a point  $\bar{x}$  in the  $B$ -frame and then to  $\bar{x}'$  in frame II. Finally we take  $x'$  by the inverse transformation to the  $A$ -frame. The result is

$$x' = R_{-\alpha}R_{\beta_2}L_1R_{\alpha}(x + a - b) + b - a \quad (2)$$

On the way across  $A$  we find

$$x' = R_{-\alpha}R_{\alpha_3}L_1R_{\alpha}x.$$

Therefore we read off

$$R_{-\alpha}R_{\alpha_3}L_1R_{\alpha} = R_{-\alpha}R_{\beta_2}L_1R_{\alpha} \quad (3a)$$

$$R_{-\alpha}R_{\beta_2}L_1R_{\alpha}(a - b) = a - b. \quad (3b)$$

The first equation gives  $\alpha_3 = \beta_2$ . The second equation tells that the edge  $\overline{AB}$  is an eigenvector of the Lorentz transformation  $R_{\beta_2}L_1$  with eigenvalue 1. This is nothing but the information that all points on this edge are fixed points under the transformation. That is, given the transformation law and given that there is one and only one frame attached to every polygon we get the result that 't Hooft's polygon approach only allows for regular polygons in the pure gravity case. All angles in a polygon have to be equal. In particular that would mean given the boosts at any node in any polygon, all the angles and all the boosts in the whole universe are given by the vertex equations. As an aside we also like to comment on the quasistatic vertex. There one angle is forced to be equal to  $\pi$ . By the result above all angles within the polygon would have to be equal to  $\pi$ . As our polygons have to close we get the result that the quasistatic vertex in the pure gravity case would be a possible configuration in closed universes only, but not in open ones.

We conclude that it is too restrictive to assume that there is one and only one coordinate system attached to every polygon. Depending on which vertex gets involved in the transformation from one polygon to an adjacent one we have to allow for frames which are rotated relative to each other.

### 3 Tessellated Particle Universes in (2+1)D

We now couple point particles to (2+1)D gravity. The resulting equations of motion are exactly solvable and lead to a conical structure of space-time. The

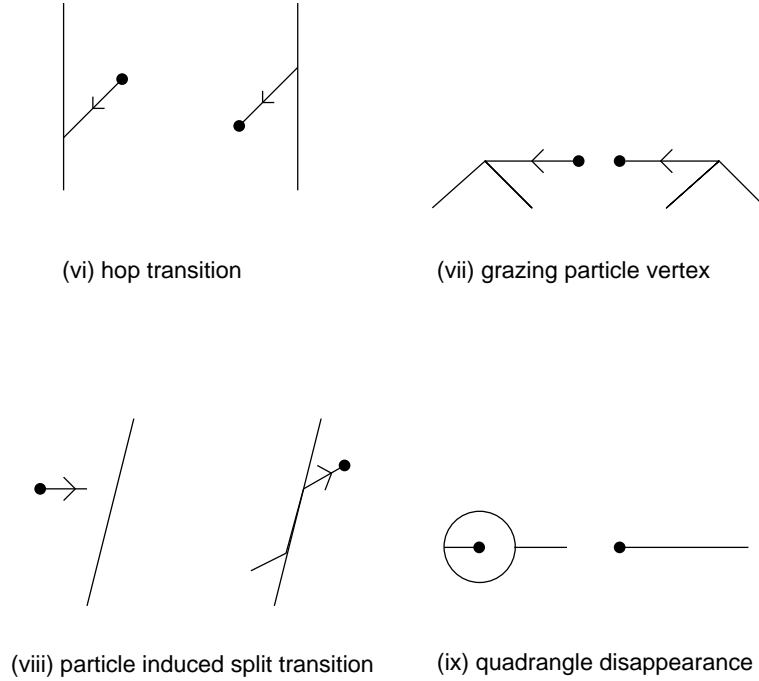


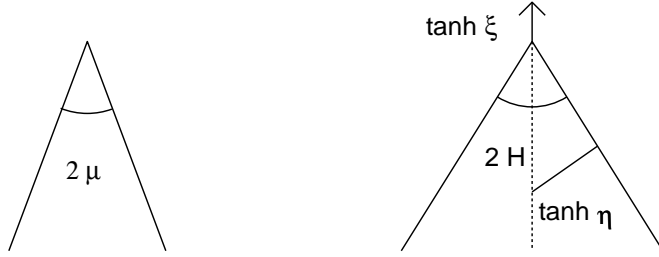
**figure 6:** particle transitions

angle of the cone is proportional to the mass of the particle which is restricted by the equations of motion to  $0 \leq m \leq 1/4G$  in the one particle case<sup>5</sup> Many-body sources can have higher mass [14].

If we project the gravitational field of a point particle onto the 2D Cauchy surface, the particle cuts out a wedge of the 2D hypersurface. The two sides of this wedge are identified. As the space-time between the particles still remains flat all particles have to be at vertex points. Besides the vacuum transitions so called particle transitions have to be taken into account. They have been classified by 't Hooft [9] and are shown in **figure 6**.

If we consider an edge ending in a particle, i.e. a 1-valent particle vertex, the vertex equations get replaced by the particle equations. These particle consistency equations also have been introduced in the paper [9]. They are derived by geometrical considerations (see **figure 7**). Let us denote by  $2\mu$  the angle of the wedge cut by the static particle in the 2D spatial hypersurface. Now we assume that the particle is moving with a velocity  $v = \tanh \xi$ , where  $\xi$  is the Lorentz boost parameter, in the direction of the bisector of the wedge. Due to the motion of the particle the wedge gets a velocity  $\tanh \eta$  as well. By Lorentz contraction the wedge widens. We denote the angle by  $2H$  and read from **figure 7** (ii)

<sup>5</sup>whenever the mass exceeds this limit the high mass particle sitting at the origin can be transformed into one with a mass within the range  $0 \leq m \leq 1/4G$  sitting at  $\infty$ .



(i) the static particle

(ii) the moving particle

**figure 7:** particle equations

$$\tanh \xi \sin H = \tanh \eta. \quad (4)$$

Combination of **figure 7** (i) and (ii) yields

$$\tan H = \tan \mu \cosh \xi. \quad (5)$$

From (4) and (5) the equations

$$\cos \mu = \cos H \cosh \eta \quad (6)$$

$$\sinh \eta = \sin \mu \sinh \xi \quad (7)$$

can be derived. Equation (4) relates the boost velocity  $\tanh \eta$  and the velocity of a vertex  $\tanh \xi$ .  $H$  is half the deficit angle. That means whenever there is a boost neither the deficit angle nor the velocity of the vertex can be zero. If one assigns a mass to a vertex, a deficit angle at rest can be obtained by equation (6). These equations are used to calculate proper initial configurations and new sets of data after a particle involved transition takes place.

Let us now define an angle  $\hat{H}$  by setting  $H = \pi/2 + \hat{H}$ . This implies  $\sin H = \sin \pi/2 \cos \hat{H} = \cos \hat{H}$ . In terms of the new quantity  $\hat{H}$  equation (4) becomes

$$\tanh \eta = \cos \hat{H} \tanh \xi \quad (8)$$

This equation and equation (7) are nothing but the defining equations for a rectangular triangle in hyperbolic space, i.e.  $\hat{H}, \mu, \xi$  may be interpreted as angles and edges in a rectangular triangle in hyperbolic geometry. This is illustrated in **figure 8**. Two entities completely determine the triangle. Hence either  $\eta$  and  $\hat{H}$  or  $\eta$  and  $\xi$  can be chosen.

The particle could also be located at a 3-valent vertex, leading to different consistency equations. The presence of a particle curves the spacetime. That is, the vertex with its three joining edges is no longer in a flat 2D spatial hypersurface but is located on a cone. Let us first consider the case where the particle is at rest as illustrated in **figure 9**. The points  $A$  and  $A'$  are identified by a linear transformation. That means in this context that the sines of two

angles  $\theta$  and  $\theta'$  are equal if  $\theta$  and  $\theta'$  differ by multiples of  $2(\pi - \mu)$ . From this one can calculate the transformation from an angle  $\alpha'$  in the plane to an angle  $\alpha$  on the cone,  $\alpha' = c\alpha$ .  $c \in \mathbb{R}$  is the set of all linear transformations

$$\sin 2c(\pi - \mu) = 1 \quad (9)$$

$$\implies 2c(\pi - \mu) = 2\pi k, \quad k \in \mathbb{Z} \quad (10)$$

$$\implies c = \frac{\pi}{\pi - \mu} k, \quad k \in \mathbb{Z} \quad (11)$$

If at a point  $P$  with mass  $m$  there meet three vertices with angles  $\alpha_1, \alpha_2, \alpha_3$ , where  $\alpha_i$  denotes the angle in a reference frame of an origin with mass zero the new consistency conditions are given by

$$L_2 R'_3 L_1 R'_2 L_3 R'_1 = \mathbb{1}, \quad (12)$$

where  $R'_i$  denotes a rotation by  $\alpha'_i = \frac{\pi}{\pi - \mu} \alpha_i$ . In the limit  $\mu \rightarrow 0$  we find  $\lim_{\mu \rightarrow 0} \alpha'_i = \alpha_i$ . The boosts  $\eta_i$  of the edges are not changed.

Let us now consider the case of a moving vertex with mass  $m > 0$ . There is a boost  $\eta$  and equation (5) holds. The angle  $\mu$  is boosted by the velocity  $\tanh \eta$  to become the angle  $H$ . This gives

$$L_2 R'_3 L_1 R'_2 L_3 R'_1 = L_\eta, \quad (13)$$

In the limit of vanishing velocity we have  $\eta \rightarrow 0$  and one obtains the equation (12) again. In the limit of vanishing mass the angle  $\mu$  is zero as well and we are back to the situation without a particle, i.e. the massless vertex. Note that (13) is not very different from the case where the particle is at rest. The boost  $L_2$  is reduced by  $\eta$ :

$$L_\eta^{-1} L_2 R'_3 L_1 R'_2 L_3 R'_1 = \mathbb{1}.$$

As this equation holds for all cyclic permutations of the indices 1, 2, 3 the assertion is true for the boosts  $L_1$  and  $L_3$  as well

$$L_\eta^{-1} L_3 R'_1 L_2 R'_3 L_1 R'_2 = \mathbb{1}.$$

$$L_\eta^{-1} L_1 R'_2 L_3 R'_1 L_2 R'_3 = \mathbb{1}.$$

Using these three equations to solve for  $\eta_1, \eta_2$  and  $\eta_3$  in terms of the angles shows that the boost due to the particle is no longer observed at 3-valent vertices (although of course its effect is seen in the angle  $H$ ).

The equations of motion of the polygon tessellated universe have to be supplemented by another growth rate. An edge connects two vertices at which there is either a particle or there is none. The growth rate associated with the moving particle can be calculated as follows (**figure 10**).

Assume a particle with mass  $m$  is moving with constant velocity in the negative  $x$ -direction. Due to the mass of the particle and the motion it cuts out a wedge of the 2D spatial hypersurface with an angle  $2H$  at a given time  $t$ . At another instant of time, say  $t + dt$ , the wedge is translated in the direction of motion by an amount  $\tanh \xi dt$ . The growth rate is then

$$g_P = \tanh \eta \cot H = \tanh \xi \cos H.$$

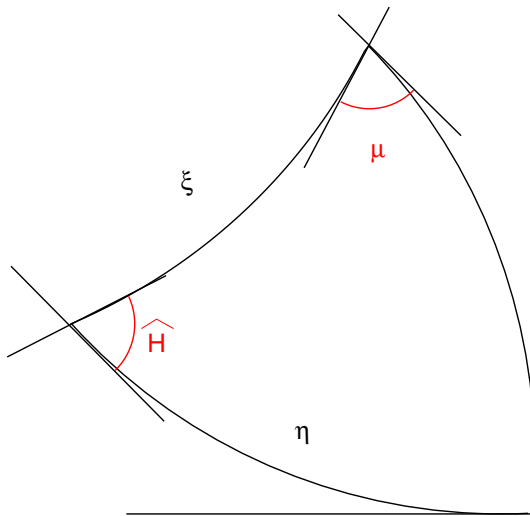


**figure 8:** hyperbolic geometry in the particle context

## 4 Some Initial Configurations

At first we confine ourselves to pure gravity initial configurations and in particular to regular ones only. The consistency equations restrict the possible sets of data severely.

In the following illustrations we have shown the Euclidean edge lengths and angles instead of the hyperbolic shapes only. All figures represent 3D geometries. **Figure 11** shows a tetrahedral configuration drawn from the top. All boosts and all angles are equal. In **figure 12** the configuration is cubical. The rectangles on the top and bottom are of equal size. In the figure one of them is drawn smaller in order to show the vertical edges. Neither the angles nor the edges need to be of equal size. **Figure 13** and **figure 14** differ from **figure 12** by the shape of the top and the bottom polygon. In **figure 13** the base polygon is a triangle and in **figure 14** it is a pentagon. The restrictions on the angles and the boost parameters are found in the illustration. Thus we have introduced initial configurations with an even and an odd number of edges.

Now we like to present initial data for regular and distorted particle universes. We place at every vertex  $A, B, C, D$  of the tetrahedron (see **figure 15**) a particle with mass  $m_i$  and velocity  $v_i$ ,  $i = A, B, C, D$ . The deficit angles  $H_A, H_B, H_C$  and  $H_D$  are then given by (5), where  $\mu_i = \pi m_i$  and  $\cosh \xi = (1 - v_i^2/c^2)^{-1/2}$ .  $c$  denotes the velocity of light. At the vertex  $A$  we choose all angles  $\alpha_{A,j}$ ,  $j = 1, 2, 3$  on the cone to be equal and calculate the angles  $\alpha'_j$ .  $\alpha'_{A,j}$  are the angles which correspond to  $\alpha_{A,j}$  in the massless situation, i.e.  $\alpha'_{A,j} = \frac{\pi}{\pi - H_A} \alpha_{A,j}$ . The boosts  $\eta_{AB}, \eta_{AC}$  and  $\eta_{AD}$  follow from equation (A.4) where the angles  $\alpha_j$  are replaced by the angles  $\alpha'_j$ . At vertex  $B$  the boost  $\eta_{AB}$  is already known. The angles  $\alpha_{CBA}, \alpha_{ABD}$  are chosen arbitrarily, the corresponding angles  $\alpha'_{CBA}, \alpha'_{ABD}$  are

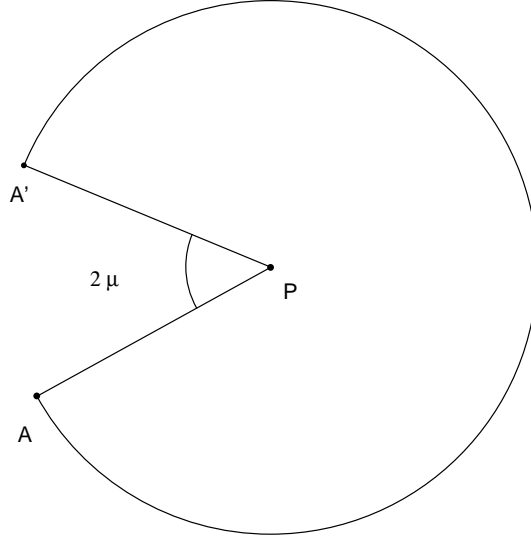


figure 9: particle vertex at rest

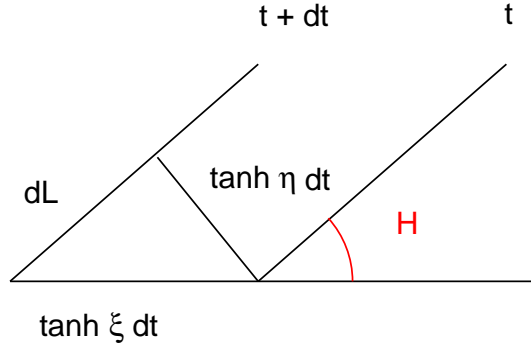
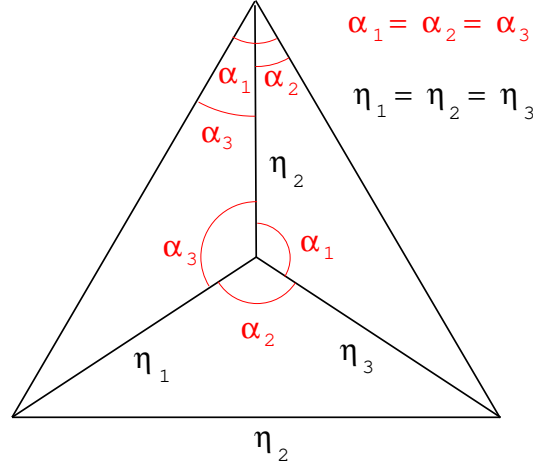


figure 10: particle equations of motion

calculated. The angle  $\alpha'_{DBC}$  then the boosts  $\eta_{BC}$  and  $\eta_{BD}$  follow using the modified equation (A.4). At  $C$  the boosts  $\eta_{AC}$  and  $\eta_{BC}$  are fixed. We can only give data for the angle  $\alpha_{ACB}$ .  $\eta_{CD}$ ,  $\alpha'_{DCB}$  and  $\alpha'_{DCA}$  follow from the modified equation (A.5). At  $D$  all boosts are known and all angles have to be computed from (A.5).

The numerical data for one of these distorted 4-particle tetrahedron configurations is included in **table 1**.

The completely regular tetrahedron is a special case of the situation described above. Setting the masses of the particles  $m = 1/4$ , the velocities  $v = \sqrt{3}/2 c$  and the angles on the cone  $\alpha = 90^\circ$ , one finds the deficit angles  $H = 63.43^\circ$ , the angles  $\alpha' = 138.98^\circ$ , and the boosts  $\eta = 0.89$ .



**figure 11:** initial configuration I

Vertex	A	B	C	D
Mass	$m_A = 0.1$	$m_B = 0.15$	$m_C = 0.2$	$m_D = 0.25$
Velocity	$v_A = 0.5 c$	$v_B = 0.6 c$	$v_C = 0.4 c$	$v_D = 0.45 c$
Deficit angle	$H_A = 20.57$	$H_B = 32.49$	$H_C = 38.40$	$H_D = 48.23$
Observed angles	$\alpha_{CAD} = 115.00$ $\alpha_{DAB} = 115.00$ $\alpha_{BAC} = 115.00$	$\alpha_{DBC} = 111.59$ $\alpha_{CBA} = 105.00$ $\alpha_{ABD} = 105.00$	$\alpha_{BCD} = 94.02$ $\alpha_{DCA} = 77.65$ $\alpha_{ACB} = 125.00$	$\alpha_{CDB} = 87.50$ $\alpha_{BDA} = 116.32$ $\alpha_{ADC} = 72.26$
Angles for calculation	$\alpha'_{CAD} = 129.83$ $\alpha'_{DAB} = 129.83$ $\alpha'_{BAC} = 129.83$	$\alpha'_{DBC} = 136.18$ $\alpha'_{CBA} = 128.13$ $\alpha'_{ABD} = 128.13$	$\alpha'_{BCD} = 119.53$ $\alpha'_{DCA} = 98.71$ $\alpha'_{ACB} = 158.90$	$\alpha'_{CDB} = 119.53$ $\alpha'_{BDA} = 158.90$ $\alpha'_{ADC} = 98.71$
Boosts	$\eta_{AB} = 0.59$ $\eta_{AC} = 0.59$ $\eta_{AD} = 0.59$	$\eta_{AB} = 0.59$ $\eta_{BC} = 0.64$ $\eta_{BD} = 0.64$	$\eta_{AC} = 0.59$ $\eta_{BC} = 0.64$ $\eta_{CD} = 0.29$	$\eta_{AD} = 0.59$ $\eta_{BD} = 0.64$ $\eta_{CD} = 0.29$

**table 1 :** Data for a distorted 4-particle tetrahedron universe

## Acknowledgment

One of the authors (H. H.) is indebted to G. 't Hooft, W. Gleißner, R. Ionicioiu, and M. Welling for discussions on the subject. The work has been supported in part by the UK Particle Physics and Astronomy Research Council.

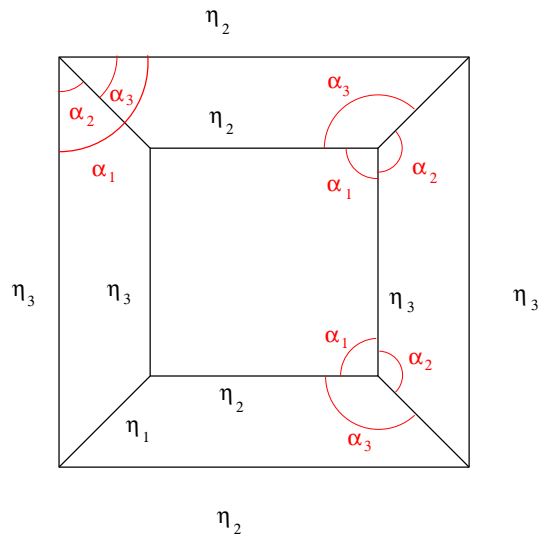


figure 12: initial configuration II

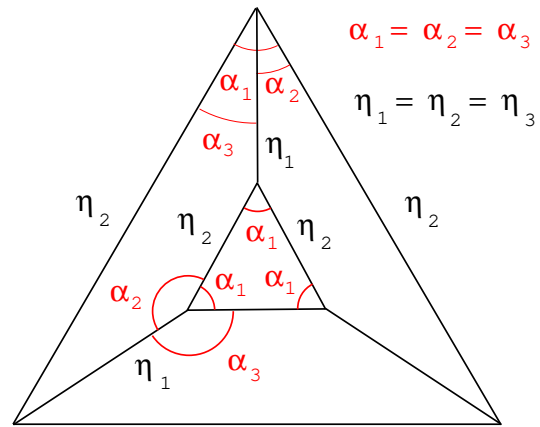


figure 13: initial configuration III

## References

- [1] Greenberg M. J. : *Euclidean and Non-Euclidean Geometries*. W. H. Freeman (1980).
- [2] Gott J. R.: *Phys. Rev. Lett.* **66**, 1126 (1991).
- [3] Carlip S.: Lectures on (2+1)-Dimensional Gravity, gr-qc/9503024.
- [4] Waelbroeck H.: Canonical Quantization of (2+1)-Dimensional Gravity, *Phys. Rev.* **D50**, 4982–4992 (1994).
- [5] Waelbroeck H., Zapata J.A.: 2+1 Covariant Lattice Theory and 't Hooft's Formulation, *Class. Quant. Grav.* **13**, 1761 – 1768 (1996).
- [6] Welling M.: The Torus Universe in the Polygon Approach to 2+1-Dimensional Gravity, *Class. Quant. Grav.* **14**, 929 – 943 (1997).
- [7] Matschull H.J., Welling M.: Quantum Mechanics of a Point Particle in (2+1)-Dimensional Gravity, gr-qc/9708054.
- [8] Welling M., Bijlsma M.: Pauli-Lubanski Scalar in the Polygon Approach to 2+1-Dimensional Gravity, *Class. Quant. Grav.* **13**, 1769 – 1774 (1996).
- [9] 't Hooft G.: Causality in (2+1)-Dimensional Gravity, *Class. Quant. Grav.* **9**, 1335–1348 (1992).
- [10] 't Hooft G.: The Evolution of Gravitating Point Particles in 2+1 Dimensions, *Class. Quant. Grav.* **10**, 1023–1038 (1993).
- [11] 't Hooft G.: Canonical Quantization of Gravitating Point Particles in 2+1, *Class. Quant. Grav.* **10**, 1653–1664 (1993).
- [12] 't Hooft G.: Classical N-Particle Cosmology in 2+1 Dimensions, *Class. Quant. Grav.* **10**, S79–S91 (1993).
- [13] 't Hooft G.: Quantization of Point Particles in (2+1)-Dimensional Gravity and Spacetime Discreteness, *Class. Quant. Grav.* **13**, 1023–1039 (1996).
- [14] Deser S., Jackiw R., 't Hooft, G.: Three-Dimensional Einstein Gravity: Dynamics of Flat Space, *Ann. Phys.* **152**, 220–235 (1984).
- [15] Franzosi R., Guadagnini E.: Topology and Classical Geometry in (2+1) Gravity, *Class. Quant. Grav.* **13**, 433–460 (1996).
- [16] Franzosi R., Guadagnini E.: Particle Decays and Space-Time Kinematics in (2+1) Gravity, *Nucl. Phys.* **B450**, 327–354 (1995).

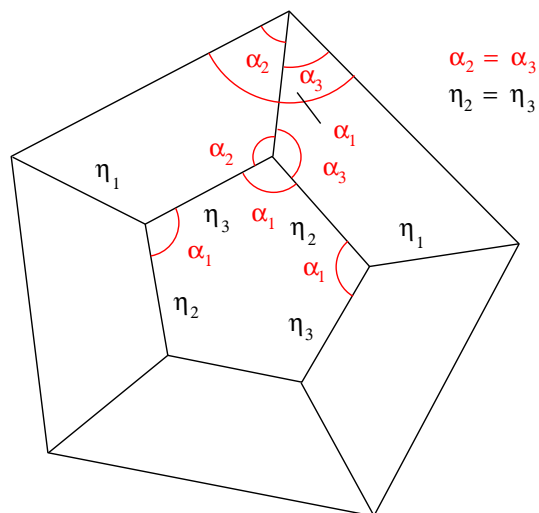


figure 14: initial configuration IV

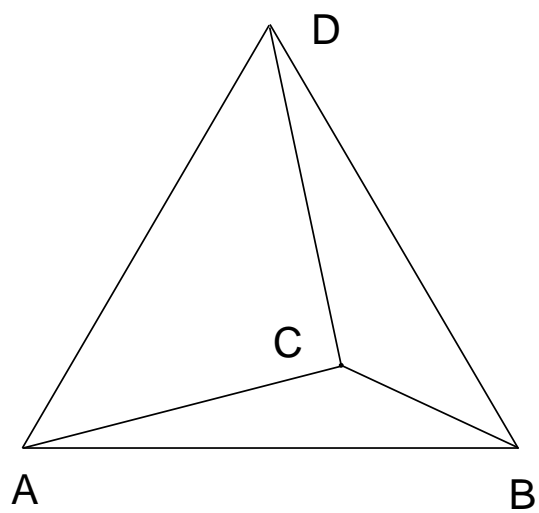


figure 15: distorted tetrahedron